Article published online: 2024-09-09

The Study of Calcium Chloride Effect on Silver Nanoparticles Capping with Roselle Extract Granule against *Aggregatibacter actinomycetemcomitans*

Thanaphoom Chaiwong[1,2] Ichaya Yiemwattana[3] Sasitharee Nathamtong[3] Tipruthai Prayoonwong[3] Suttimas Yuakyong[4] Sirorat Wacharanad[3]

[1] Faculty of Dentistry, Naresuan University, Phitsanulok, Thailand
[2] Phayao Provincial Public Health Office, Phayao, Thailand
[3] Department of Preventive Dentistry, Faculty of Dentistry, Naresuan University, Phitsanulok, Thailand
[4] Research and Innovation Division, Faculty of Dentistry, Naresuan University, Phitsanulok, Thailand

Address for correspondence Sirorat Wacharanad, DDS, PhD, Department of Preventive Dentistry, Faculty of Dentistry, Naresuan University, Phitsanulok, Thailand (e-mail: sirorat.w@gmail.com).

Eur J Gen Dent

Abstract

Objectives The primary aim of this research is to investigate the influence of calcium chloride on the synthesis of silver nanoparticles coated with roselle extract and enclosed within alginate and calcium chloride (SNP-Ro-$CaCl_2$) beads, designated as SNP-Ro-$CaCl_2$ beads. Additionally, the study aims to assess their antimicrobial activity.

Materials and Methods For the preparation of SNP-Ro-$CaCl_2$ beads, SNPs and alginate gel were mixed, followed by dropping in three different concentrations of $CaCl_2$ solution (1%, 3%, and 5% w/v). The morphological structure of the SNP-Ro-$CaCl_2$ beads was analyzed using a stereoscope and scanning electron microscope (SEM). Over a period of 14 days, the release of SNPs was monitored using ultraviolet-visible (UV-Vis) spectroscopy. Additionally, the activity against *Aggregatibacter actinomycetemcomitans* was evaluated using the disk diffusion technique.

Statistical Analysis The data for this experiment were analyzed using one-way analysis of variance (ANOVA) and Scheffe's method.

Results The results revealed that varying concentrations of calcium chloride had distinct crosslinking effects on alginate, resulting in different voids and porosity within the SNP-Ro-$CaCl_2$ beads. In the SNP-Ro-1% $CaCl_2$ beads, the inner element exhibited higher porosity, facilitating faster activation and greater efficiency in releasing SNPs. Regarding activity against *A. actinomycetemcomitans* after 14 days, SNP-Ro-1% $CaCl_2$ beads showed a larger inhibition zone diameter compared to other concentrations, while no statistically significant difference in the inhibition zone diameter was observed between SNP-Ro-3% $CaCl_2$ and SNP-Ro-5% $CaCl_2$ beads. Additionally, it was observed that the antimicrobial effectiveness diminished after 17 days through testing of the lifetimes of the three concentrations.

Keywords

- *Aggregatibacter actinomycetemcomitans*
- antimicrobial
- calcium chloride
- disk diffusion method
- microwave-assisted synthesis
- periodontal therapy
- silver nanoparticles

DOI https://doi.org/10.1055/s-0044-1787793.
ISSN 2320-4753.

Thieme Medical and Scientific Publishers Pvt. Ltd., A-12, 2nd Floor, Sector 2, Noida-201301 UP, India

Conclusions This study developed a method for depositing SNP-Ro into alginate gel and crosslinking it with $CaCl_2$ to produce small beads for the sustained release of SNP-Ro in periodontal lesions. Consequently, the SNP-Ro-$CaCl_2$ beads have the potential to be developed as adjunctive locally delivered antimicrobial agents in periodontal therapy.

Introduction

Periodontal disease is an inflammatory disease that is caused by dental biofilm. These inflammations are involved with the gingiva, periodontal ligament, cementum, and alveolar bone. Gingivitis, which is inflamed gingival tissue only, is found in the general population. If the bacteria rapidly increase or the host has low immunity, it will destroy the other periodontal tissue and develop into periodontitis, which is inflammation that destroys all the periodontal tissue, and the teeth will be lost. Cleaning in this area is restricted for patients with deep periodontal pocket depth. In addition, flossing and interdental brushing will be difficult in terms of cleaning in the molar tooth areas.[1,2] Thus, these patients do not use tools to clean between the teeth regularly and thoroughly. As for scaling and root planing, it is an important and standard mechanical method,[3] but there are restrictions on accessing the root of some teeth for cleaning. Therefore, it is not possible to eliminate all pathogenic microorganisms.[4,5] For this reason, antimicrobial agents are added to enhance the effective treatment of periodontal disease.

Antimicrobial agents used for periodontal disease are classified according to their method of use, including systemic and topical antimicrobials. Topical antimicrobial agents are used for direct application where you want the drug to work. The drug concentration in the periodontal sulcus is higher than that of systemic antimicrobials; thus, less of the medication must be used in order to reduce the adverse effects of drug use, such as drug resistance and drug allergies.[6] Nowadays, nanotechnology is increasingly being used in antimicrobial production. Silver nanoparticles (SNP) have very specific properties, such as good chemical stability, thermal conductivity, and electrical conductivity. SNP is the nanometer size, which will increase the surface area and can penetrate into the cell membranes of microorganisms and thus help resist bacteria, viruses, and fungi.[7] Moreover, it has been found that there are more patients who are resistant to antibiotic drugs. SNP is able to kill microorganisms without detecting drug resistance. Three methods can be used to synthesize SNP. The first is the physical method, which involves breaking down the massive material into smaller particle sizes by breaking it down from bulk to size. The other two techniques, which include chemical and biological ones, are synthetic and start with the fusion of small groups of atoms to produce new nuclei that are then developed into nanoparticles. Since the biological approach is synthetic and does not include chemicals, the environment is not exposed to any new toxins.[8] It involves the utilization of plant extracts, such as roselle,[9–11] which in this research will be used in the synthesis of SNP and are effective in killing *Aggregatibacter actinomycetemcomitans*.

A. actinomycetemcomitans, a gram-negative bacterium, significantly contributes to the development of periodontitis. It grows poorly in ambient air but thrives in an environment with a temperature of 37°C and 5% CO_2. Colonies on agar are initially small, with a diameter of 0.5 mm after 24 hours, but may exceed 1 to 2 mm after 48 hours.[12] Previously, until 2017, *A. actinomycetemcomitans* was a major factor in aggressive periodontitis in adolescents. However, after the reclassification of periodontal disease, the perceived importance of *A. actinomycetemcomitans* decreased. Nevertheless, it remains acknowledged as a crucial bacterium in periodontitis. Apart from causing periodontal disease, it has also been found that patients with infectious endocarditis can detect the bacterium *A. actinomycetemcomitans* in the heart valve.[12] It can be concluded that this bacterium is involved in causing several significant diseases; hence, there is interest in studying substances that can inhibit this bacterium. Furthermore, *A. actinomycetemcomitans* bacteria can evade the body's defenses and infiltrate gingival tissues,[13] making traditional root planing procedures inadequate for complete elimination. Therefore, the strategic use of topical antimicrobials is crucial to preventing its spread. This aligns with the objective of our research, which aims to develop a topical antimicrobial drug for eliminating bacteria lingering in the gingival pockets.

Therefore, the authors are interested in the application of SNP coated with roselle extract (SNP-Ro) as a topical antimicrobial for the treatment of periodontal disease. In previous research, SNP-Ro was formed into films using alginate, and their antimicrobial properties against *A. actinomycetemcomitans* were studied. The results of the research showed that it can kill *A. actinomycetemcomitans* completely within 180 minutes, and this film, when in contact with the agar medium, will decompose rapidly within 24 hours. The properties of the ideal local antimicrobial agents should include a long enough release time to kill microorganisms and the ability to control the release according to the appropriate form. Therefore, the authors aimed to increase the stability of the SNP film by using a more efficient forming agent, such as calcium chloride ($CaCl_2$). It is used in the binding of alginate, which is widely applied in local drug delivery. Calcium ions (Ca^{2+}) are specific to the arrangement in alginates by binding to the positive charge of guluronate, which makes the bonding of the polymer chain stronger and more stable, thereby improving polymer stability. Therefore, in this study, the research interest was the application of $CaCl_2$ to develop the molding of SNP-Ro, which will allow for a better structure and longer release control, as well as examining their antimicrobial activity against *A. actinomycetemcomitans*.

Materials and Methods

- **Preparation of SNPs are coated with roselle extract and enclosed within calcium chloride beads (SNP-Ro-$CaCl_2$ beads).**[14] A solution of silver nitrate ($AgNO_3$) was mixed with roselle extract to make the final concentration between $AgNO_3$ and roselle extract 1:0.5. This solution was then heated in a microwave (800 W) for 5 minutes. After 24 hours, the synthesized SNP-Ro was analyzed via ultraviolet-visible (UV-Vis) spectroscopy (Model: Evolution 60S). The SNP-Ro-$CaCl_2$ beads were synthesized by mixing SNP-Ro and 10% of the alginate solution (w/v). The ingredients were dropped into the beaker of the 1, 3, and 5%w/v $CaCl_2$ solution for 5 minutes, and the granules were rinsed with deionized water. Then, these granules were placed in the dryer at 45°C for 15 minutes and kept in sealed bags at room temperature. These granules were analyzed by stereoscope and scanning electron microscope (SEM).
- **Release of SNPs.** The standard calibration curve of the SNP-Ro was analyzed via UV-Vis spectroscopy. The concentration of SNP-Ro was varied at 170, 85, 42.5, 21.25, 10.63, 5.31, and 2.65 mg/dL and measured by UV-Vis spectroscopy. The relation between the concentration and absorbance values at 400 nm was plotted. The SNP-Ro-$CaCl_2$ beads (1, 3, and 5%) were dipped into deionized water to release all of the SNP-Ro from the beads. Then, this solution was measured with UV-Vis spectroscopy at 1, 3, 5, 15, 30, 60, 120, 180, and 240 minutes, and at 24, 48, 72, 168, and 336 hours in order to analyze the absorbance value at the maximum peak of the SNP-Ro wavelength.
- **Analysis of the antimicrobial activities (disk diffusion assay).**[15] An individual colony of *A. actinomycetemcomitans* (bacterial strain: ATCC29523) was suspended in brain heart infusion (BHI) broth and incubated for 24 hours. The density of the bacterial culture was adjusted to a 0.5 McFarland standard and diluted 1:100 times in nutrient broth. *A. actinomycetemcomitans* was swabbed uniformly on the BHI agar disk. Different concentrations of the SNP-Ro-$CaCl_2$ beads were pressed into the designated positions, while 0.2% of chlorhexidine gluconate (CHX) was used as the positive control and the alginate beads were used as the negative control. The culture plates were placed in a controlled environment with a temperature of 37°C and 5% CO_2 for incubation. Afterward, we carefully measured the sizes of the inhibition zones around each well at specific time points: 24, 48, 72, 168, and 336 hours. To ensure consistency, we kept the sample at a constant temperature of 37°C and 5% CO_2 throughout the experiment.
- **Lifetime of SNP-Ro-$CaCl_2$ beads.** This experiment was conducted to test the efficacy of SNP-Ro-$CaCl_2$ beads when stored at different times in order to determine the expiration date of the SNP-Ro-$CaCl_2$ beads by using the disk diffusion method. The SNP-Ro-$CaCl_2$ beads were stored for periods of 1, 3, 10, 17, 24, and 31 days, and then they were tested by the disk diffusion method.

Results

Characterization of the SNP-Ro-$CaCl_2$ Beads

The synthesized SNP-Ro showed a specific pattern at 350 to 450 nm, which indicated the formation of the SNP (►**Fig. 1B**). The plasmon resonance band spectra displayed specific peaks at 400 nm. When the SNP-Ro was fabricated with the alginic acid and three concentrations of $CaCl_2$ in the beads, it was found that the beads had a circular shape and a yellow color. The mean diameters of the SNP coated with roselle extract and enclosed within 1% $CaCl_2$ beads (SNP-Ro-1% $CaCl_2$ beads), the SNP coated with roselle extract and enclosed within 3% $CaCl_2$ beads (SNP-Ro-3% $CaCl_2$ beads), and the SNP coated with roselle extract and enclosed within 5% $CaCl_2$ beads (SNP-Ro-5% $CaCl_2$ beads) were 3.83 ± 0.02, 3.83 ± 0.12, and 3.84 ± 0.09 mm, respectively. Using the stereoscope to examine the SNP-Ro-$CaCl_2$ beads showed that the morphology of the beads presented a smooth and yellowish surface. The opacity of the SNP-Ro-$CaCl_2$ beads increases with higher $CaCl_2$ concentrations (►**Fig. 1A**). When the SNP-Ro-$CaCl_2$ beads were cut in half, it was found that the SNP-Ro-1% $CaCl_2$ beads are characterized by opacity at the edges rather than at the center, which showed a clear area, different from the SNP-Ro-3% $CaCl_2$ beads and SNP-Ro-5% $CaCl_2$ beads, which had more opacity and an opaque area extending to the center. This indicates that there is a crosslinking of $CaCl_2$ with the alginate that is greater than that in the SNP-Ro-1% $CaCl_2$ beads, as shown in ►**Fig. 1C**. This is consistent with the outer surface analysis of SNP-Ro-$CaCl_2$ beads under SEM, which found that the surface of the SNP-Ro-1% $CaCl_2$ beads showed that the presence of $CaCl_2$ was less dense than the SNP-Ro-3% $CaCl_2$ beads as well as a very high density of $CaCl_2$ at the SNP-Ro-5% $CaCl_2$ bead surface, as shown in ►**Fig. 2A–C**. When the cross-sectional analysis of SNP-Ro-1% $CaCl_2$ beads was conducted, it was found that the crosslinking of $CaCl_2$ with alginate mixed with SNP forms a typical porous appearance, as shown in ►**Fig. 2D**, and SEM at 10,000X magnification showed the appearance of SNP inside the pores of all of the 1, 3, and 5% SNP-Ro $CaCl_2$ beads (►**Fig. 2E–G**).

Release of Silver Nanoparticles

The standard calibration curve of the SNP-Ro is shown in ►**Fig. 3**. The straight-line equation representing the SNP-Ro standard calibration curve is shown below, which was used to determine the concentration of SNP-Ro to be released from the SNP-Ro-$CaCl_2$ beads:

$$y = 0.0011x + 0.0005. \quad (1)$$

The concentrations of SNP-Ro released from the SNP-Ro-$CaCl_2$ beads at 1, 3, 5, 15, 30, 60, 120, 180, and 240 minutes, and at 24, 48, 72, 168, and 336 hours are shown in ►**Fig. 4**. It was found that the SNP-Ro-1% $CaCl_2$ beads released more SNP-Ro and the release was faster than the other SNP-Ro-$CaCl_2$ beads, which initially released less and more slowly. Following this, a steady onset of SNP-Ro release was observed

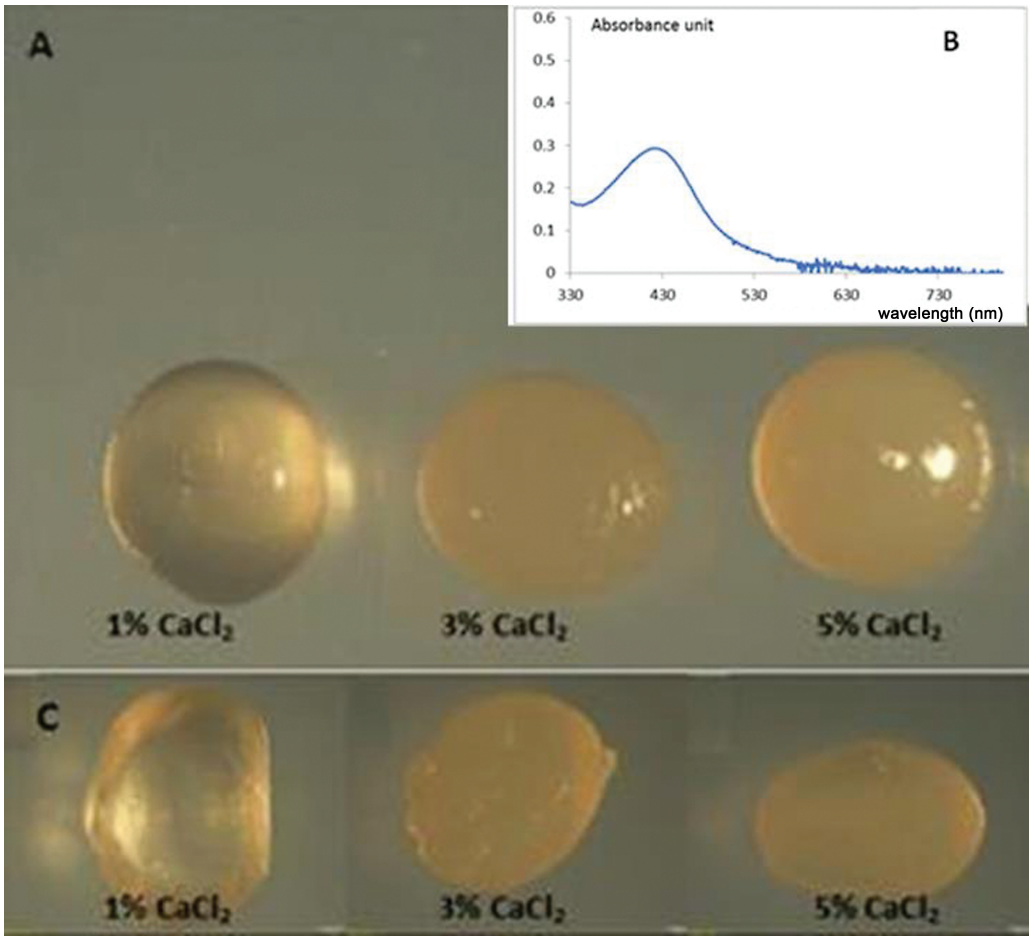

Fig. 1 (**A**) The morphological characteristics of the silver nanoparticles coated with roselle extract and enclosed within alginate and calcium chloride (SNP-Ro-$CaCl_2$) beads were analyzed via the stereoscope. (**B**) Ultraviolet (UV) visible absorbance peaks of the synthesized SNP-Ro showed a specific pattern at 350 to 450 nm, which indicated the formation of the SNP. (**C**) Stereoscopic image (5.75X magnification) showing the cross-sectional image of SNP-Ro beads synthesized in different concentrations of $CaCl_2$.

at 5 hours, in which the SNP-Ro-5% $CaCl_2$ beads released the least amount of SNP-Ro and required a longer time. Therefore, when the concentration of $CaCl_2$ was increased, a smaller amount of SNP-Ro was released and a longer period of time was needed. After 14 days of follow-up, there was less SNP-Ro released compared to 24 hours, when the highest amount of SNP-Ro was released from the SNP-Ro-1% $CaCl_2$ beads, followed by the SNP-Ro-3% $CaCl_2$ and SNP-Ro-5% $CaCl_2$ beads, respectively.

Antimicrobial Properties of the SNP-Ro-$CaCl_2$ Beads

From the results of the disk diffusion screening, the SNP-Ro-$CaCl_2$ beads were shown to clearly possess antibacterial properties against *A. actinomycetemcomitans* (►**Fig. 5A**). It was found that after 1 day, the size of the inhibition zone of SNP-Ro-1% $CaCl_2$ was 10.96 ± 0.35 mm, and there was no significant difference in the inhibition zone ($p \geq 0.05$) after 14 days. When comparing the intergroup statistics, it could be seen that the diameter of the inhibition zone of the SNP-Ro-1% $CaCl_2$ beads differs from that of the SNP-Ro-3% $CaCl_2$ and the SNP-Ro-5% $CaCl_2$ beads at a statistically significant level ($p < 0.05$). For the size of the inhibition zone after 1 day, the SNP-Ro-3% $CaCl_2$ beads and SNP-Ro-5% $CaCl_2$ beads had a size of 7.57 ± 0.85 and 7.95 ± 0.40 mm, respectively. When comparing the statistics between groups, it was found that both groups were not significantly different in terms of inhibition zone size ($p \geq 0.05$). After 14 days, statistical comparisons were made within the group. There was no statistically significant difference ($p \geq 0.05$) compared to the first day. Compared to the negative control group, for the alginate beads, an inhibition zone was not found at all. Compared with the positive control group (0.2% CHX chip in the amount of 0.1 mL), the inhibition zone was 15.44 ± 0.12 to 16.07 ± 0.03 mm. It can be concluded that all three types of SNP-Ro-$CaCl_2$ beads are most effective against *A. actinomycetemcomitans* in 24 hours. After 14 days, there was no difference in the results. The SNP-Ro-1% $CaCl_2$ beads were the most effective against *A. actinomycetemcomitans*.

Study on the Effect of SNP-Ro-$CaCl_2$ Beads on Inhibition of the Growth of *A. actinomycetemcomitans* When Stored for Different Periods of Time

This experiment aimed to test the efficacy of SNP-Ro-$CaCl_2$ beads formed by the disk diffusion method when stored for 1, 3, 10, 17, 24, and 31 days to determine their expiration date (►**Fig. 5B**). It was observed that SNP-Ro-1% $CaCl_2$ beads on days 1, 3, and 10 exhibited a larger diameter compared to

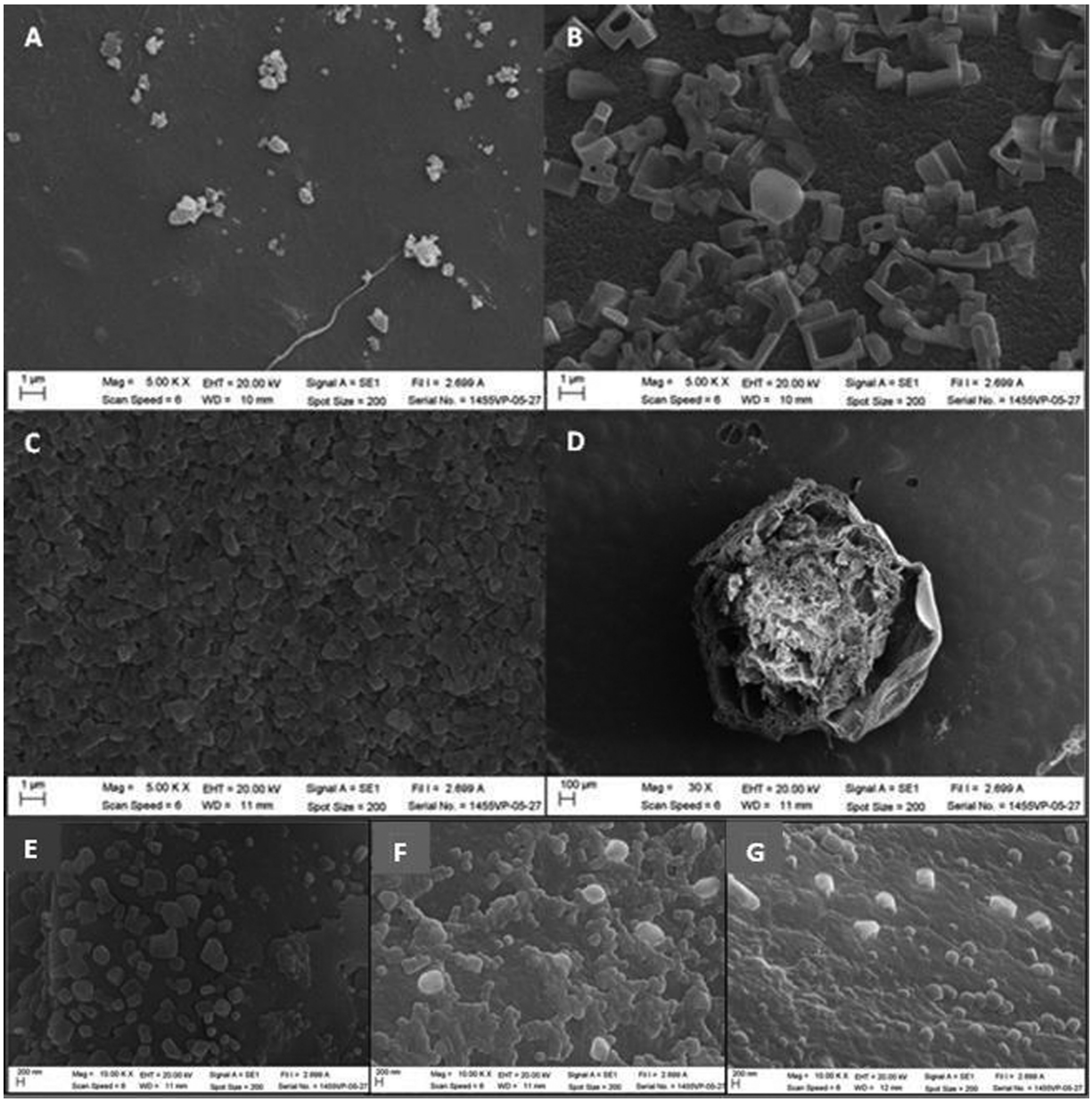

Fig. 2 A scanning electron microscope (SEM) image shows the outer surface of (**A**) silver nanoparticles coated with roselle extract and enclosed within alginate and 1% calcium chloride (SNP-Ro-1% $CaCl_2$)beads, (**B**) SNP-Ro-3% $CaCl_2$ beads, and (**C**) SNP-Ro-5% $CaCl_2$ beads at a magnification of 5,000X. (**D**) The cross-sectional image of SNP-Ro-1% $CaCl_2$ beads at 30X magnification. (**E–G**) SEM at 10,000X magnification showed the appearance of SNP inside the pores of all of the 1, 3, and 5% SNP-Ro-$CaCl_2$ beads, in sequence.

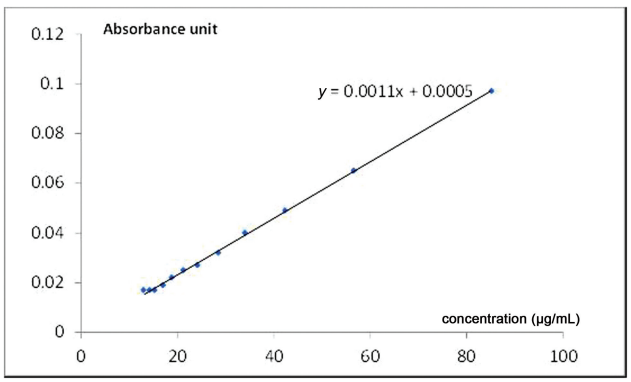

Fig. 3 Graph representing the standard calibration curve of the SNP-Ro.

those from day 17 onward, with a statistically significant difference ($p < 0.05$), indicating reduced effectiveness against *A. actinomycetemcomitans.* The inhibition zone of SNP-Ro-1% $CaCl_2$ beads was 10.96 ± 0.35 mm on the first day, decreasing to 5.21 ± 0.73 mm after 17 days. Thereafter, it showed a slight further reduction, with the inhibition zone measuring only 4.47 ± 0.19 mm after 1 month, which was not significantly different ($p \geq 0.05$) from day 17. Similar trends were observed for SNP-Ro-3% $CaCl_2$ beads, with the inhibition zone diameter being 7.57 ± 0.86 mm on the first day, reducing to 5.05 ± 0.56 mm on day 17, and measuring 3.04 ± 0.24 mm after 1 month. For SNP-Ro-5% $CaCl_2$ beads, the inhibition zone was 7.95 ± 0.40 mm on the first day,

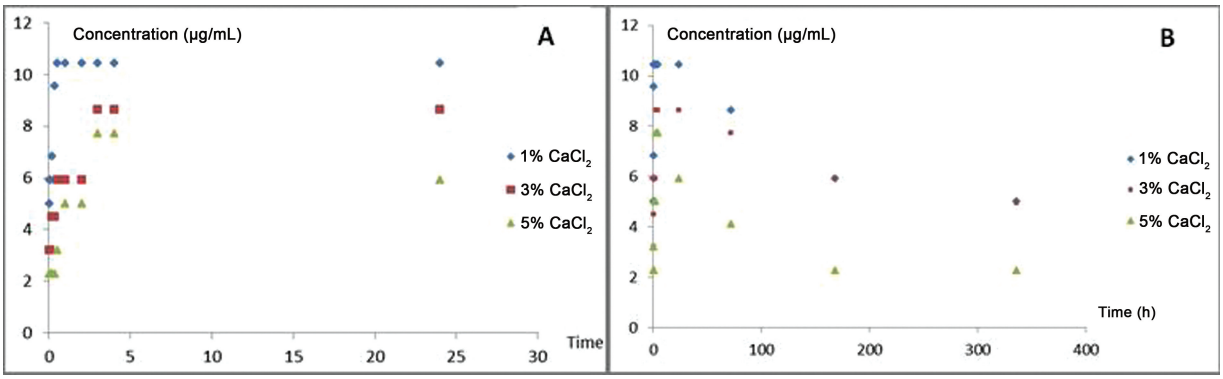

Fig. 4 (A) Graph representing the concentrations of silver nanoparticles coated with roselle extract (SNP-Ro) released from the silver nanoparticles coated with roselle extract and enclosed within alginate and calcium chloride (SNP-Ro-$CaCl_2$) beads at 1, 3, 5, 15, 30, 60, 120, 180, and 240 minutes, and at 24 hours. (**B**) Graph representing the concentrations of SNP-Ro released from the SNP-Ro-$CaCl_2$ beads at 1, 3, 5, 15, 30, 60, 120, 180, and 240 minutes and at 24, 48, 72, 168, and 336 hours.

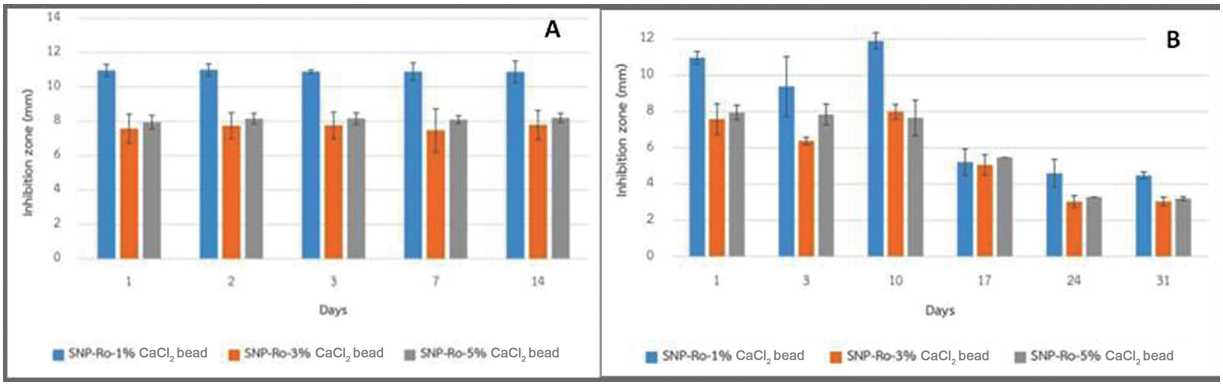

Fig. 5 (A) Graph representing the antibacterial activity of silver nanoparticles coated with roselle extract and enclosed within alginate and calcium chloride (SNP-Ro-$CaCl_2$) beads by disk diffusion assay. (**B**) Graph representing the efficacy of SNP-Ro-$CaCl_2$ beads formed by the disk diffusion method when stored at 1, 3, 10, 17, 24, and 31 days.

decreasing to 5.47 ± 0.00 mm on day 17, and further reduced to 3.20 ± 0.10 mm after 1 month.

Discussion

In relation to the findings, the SNP-Ro-$CaCl_2$ beads were synthesized through the crosslinking of $CaCl_2$ with alginate, resulting in smooth, spherical gel beads consistent with the study by Lee et al.[16] Various factors influence the size and shape of alginate beads, one of which is the concentration of $CaCl_2$. As the concentration of $CaCl_2$ increased, the alginate beads became rounder and more uniform in shape. The higher levels of calcium ions prompted tighter binding of the alginate polymer chains, resulting in smaller beads. These results differ from the findings of this study, which reported that the diameters of the three concentrations of SNP-Ro-$CaCl_2$ beads were the same. The variation in results can be attributed to the findings of Lotfipour et al,[17] who discovered that the increase in alginate affects the size of alginate granules more than changes in the concentration of $CaCl_2$. Nonetheless, in our experiment, while we increased $CaCl_2$ concentration, alginate concentration remained unchanged, resulting in minimal changes in the diameter of SNP-Ro-$CaCl_2$ beads. Similarly, the study by Szekalska et al[18] found that when the alginate structure was modified with 0.1 and 0.05% $CaCl_2$, there was no difference in the size of the alginate.

Crosslinking between $CaCl_2$ and alginate was observed in both the outer surface and cross-sectional images of the SNP-Ro-$CaCl_2$ beads using stereoscope analysis. These images revealed a smooth surface,[19,20] with the SNP-Ro-1% $CaCl_2$ beads appearing more translucent compared to the SNP-Ro-3% $CaCl_2$ and SNP-Ro-5% $CaCl_2$ beads, which exhibited more opacity and a larger cross-linking area. This observation aligns with findings by Quong et al[21] and Puguan et al,[22] who also noted the expulsion of external gelation gels similar to those in our study. The concentration levels of calcium ions and alginate on the surface area were found to be higher than those in the core area, resulting in a greater structural density on the surface. Consequently, a nonhomogeneous structure was evident, with the core area appearing looser due to the presence of large pores. Therefore, the use of $CaCl_2$ at lower concentrations led to the formation of less dense structures, resulting in a more transparent surface compared to higher concentrations of $CaCl_2$. Based on the SEM surface analysis, it was found that the concentration of $CaCl_2$ at the surface area was lower than that in the SNP-Ro-1% $CaCl_2$ beads. This finding is consistent with the research conducted by Swioklo et al,[23] which revealed that with increasing

concentrations of $CaCl_2$, calcium crystals were observed, indicating the precipitation of calcium salts during the drying process.

Additionally, when examining the release of SNP-Ro from the SNP-Ro-$CaCl_2$ beads, it was observed that the SNP-Ro-1% $CaCl_2$ beads exhibited a rapid and extensive release of SNP-Ro. Conversely, with an increase in $CaCl_2$ concentration, the release time slowed and the quantity released decreased. This observation is consistent with the findings of Szekalska et al,[18] where the use of 0.1% $CaCl_2$ to enhance alginate structure significantly increased the release of metformin, sustaining release from the first 2 hours up to 12 hours. However, the structural enhancement of alginate with 0.05% $CaCl_2$ resulted in a faster drug release. These outcomes can be attributed to higher crosslinking occurring at higher concentrations of $CaCl_2$, which acts as a mechanism to regulate drug release. This finding is supported by Russo et al[24] and Wong,[25] who observed that calcium ions interact specifically with alginate orientation, binding the cations of the guluronate similar to the arrangement of eggs in a cardboard egg carton. This enhances lateral affinity, strengthening the bonding of the polymer chain and making the polymer or alginate more stable. Consequently, it prolongs the stabilization of the drug, extending the duration of drug release. Therefore, for the release of drugs or therapeutic chemicals, the crosslinking of $CaCl_2$ with alginate would be chosen for the purpose of treatment. If a slow-release drug is desired over a longer period of time, $CaCl_2$ should be used at a high concentration. Conversely, if a quick release of the drug is desired within a short time, $CaCl_2$ should be used at a low concentration.

In the study of its antibacterial activity according to Loo et al,[26] their experiment investigated the effect of SNP synthesized using pu-erh tea leaf extract against gram-negative bacteria utilizing the disk diffusion method. The results revealed that SNP can effectively kill bacteria, generating an inhibition zone of 15 to 20 mm. In this research, the inhibition zone diminished when SNP-Ro-$CaCl_2$ beads with higher concentrations of $CaCl_2$ were employed, consistent with findings from studies on SNP-Ro release kinetics from similar bead formulations. Regarding the mechanism underlying SNP's antibacterial activity, it was observed that the compound binds to proteins, inducing structural changes in the cell membrane due to the presence of sulfur, ultimately leading to the formation of small pores. Consequently, the membrane loses its ability to regulate substance passage, culminating in cell death.[27–29] Another hypothesis posits that SNP induces alterations in the genetic code of microorganisms, rendering them incapable of cell division.

Assessing the efficacy of SNP-Ro-$CaCl_2$ beads over varying storage periods, it was observed that after 17 days, the effectiveness of these beads decreased by 50%. Consequently, measures need to be taken at this juncture to preserve their efficacy, either through the development of preservation methods to prolong the drug's effectiveness or through the steps in synthesis with reduced moisture of the beads, thus extending their shelf life.

Limitations

This research investigated the efficacy of silver beads against *A. actinomycetemcomitans*. Due to time constraints, only one type of pathogen could be studied. Culturing and testing *A. actinomycetemcomitans* are not complicated processes and do not require special equipment. Additionally, they are inexpensive. Therefore, we have chosen to conduct our initial testing with this pathogen. Further research should delve into its efficacy against other pathogens, such as *Porphyromonas gingivalis* and *Prevotella intermedia*. The cultivation of this pathogen necessitates specialized equipment, and the procedures involved are notably complex. Furthermore, it was found that there is also an issue regarding the storage of SNP so that they can maintain their efficacy for a longer period. This aspect needs to be addressed in future research endeavors.

Conclusion

Different concentrations of $CaCl_2$ result in different voids and porosity of SNP-Ro-$CaCl_2$ beads, which affect the control of the SNP-Ro release by SNP-Ro-$CaCl_2$ beads. This is due to SNP-Ro-1% $CaCl_2$ beads being highly porous, enabling fast and high-volume release of SNP-Ro. Correspondingly, the antimicrobial activity against *A. actinomycetemcomitans* at 24 hours had a greater diameter of the inhibition zone than other concentrations. When the lifetime testing was performed for all three concentrations of SNP-Ro-$CaCl_2$ beads, it was found that after 17 days, the antimicrobial efficacy was decreased. At this point, this is an opportunity to develop further research in order to obtain improved performance of SNP-Ro-$CaCl_2$ beads that have a longer life. From this experiment, researchers can develop local drug delivery optimized for controlled release by selecting the timing and dose of the drug to be released for gingival sulcus. Therefore, in further experiments, this work can be used as a model for the development of a suitable drug for the treatment of periodontal disease.

Funding
This research was supported by the Faculty of Dentistry, Naresuan University.

Conflict of Interest
None declared.

References

1 Chen M-S, Rubinson L. Preventive dental behavior in families: a national survey. J Am Dent Assoc 1982;105(01):43–46
2 Jamjoom HM. Preventive oral health knowledge and practice in Jeddah, Saudi Arabia. Magalat Game'at al-Malik Abdul Aziz Al-U'lum al-Tibyat 2001;9:17–25
3 Zafar MS. Comparing the effects of manual and ultrasonic instrumentation on root surface mechanical properties. Eur J Dent 2016;10(04):517–521
4 Jepsen S, Deschner J, Braun A, Schwarz F, Eberhard J. Calculus removal and the prevention of its formation. Periodontol 2000 2011;55(01):167–188

5 Haffajee AD, Cugini MA, Dibart S, Smith C, Kent RL Jr, Socransky SS. The effect of SRP on the clinical and microbiological parameters of periodontal diseases. J Clin Periodontol 1997;24(05):324–334
6 Etienne D. Locally delivered antimicrobials for the treatment of chronic periodontitis. Oral Dis 2003;9(Suppl 1):45–50
7 Ozak ST, Ozkan P. Nanotechnology and dentistry. Eur J Dent 2013; 7(01):145–151
8 Ahmed S, Ahmad M, Swami BL, Ikram S. A review on plants extract mediated synthesis of silver nanoparticles for antimicrobial applications: a green expertise. J Adv Res 2016;7(01):17–28
9 Wacharanad S, Taya T, Phrai-in N. The study of antimicrobial activity on *Aggregatibacter actinomycetemcomitans* of AgNPs capping with roselle. J Int Dent Med Res 2019;12(03):912–916
10 Higginbotham KL, Burris KP, Zivanovic S, Davidson PM, Stewart CN Jr. Antimicrobial activity of *Hibiscus sabdariffa* aqueous extracts against *Escherichia coli* O157:H7 and *Staphylococcus aureus* in a microbiological medium and milk of various fat concentrations. J Food Prot 2014;77(02):262–268
11 Abdallah EM. Antibacterial efficiency of the Sudanese Roselle (*Hibiscus sabdariffa* L.), a famous beverage from Sudanese folk medicine. J Intercult Ethnopharmacol 2016;5(02):186–190
12 Nørskov-Lauritsen N, Claesson R, Birkeholm Jensen A, Åberg CH, Haubek D. *Aggregatibacter actinomycetemcomitans*: clinical significance of a pathobiont subjected to ample changes in classification and nomenclature. Pathogens 2019;8(04):1–18
13 Christersson LA, Albini B, Zambon JJ, Wikesjö UME, Genco RJ. Tissue localization of *Actinobacillus actinomycetemcomitans* in human periodontitis. I. Light, immunofluorescence and electron microscopic studies. J Periodontol 1987;58(08):529–539
14 Mandal S, Kumar SS, Krishnamoorthy B, Basu SK. Development and evaluation of calcium alginate beads prepared by sequential and simultaneous methods. Braz J Pharm Sci 2010;46(04):785–793
15 Wacharanad S, Thatree P, Yiemwattana P, et al. Antimicrobial activity of roselle-capped silver nanochip on *Aggregatibacter actinomycetemcomitans*. Eur J Dent 2021;15(03):574–578
16 Lee BB, Ravindra P, Chan ES. Size and shape of calcium alginate beads produced by extrusion dripping. Chem Eng Technol 2013; 36(10):1627–1642
17 Lotfipour F, Mirzaeei S, Maghsoodi M. Evaluation of the effect of $CaCl_2$ and alginate concentrations and hardening time on the characteristics of *Lactobacillus acidophilus* loaded alginate beads using response surface analysis. Adv Pharm Bull 2012;2(01): 71–78
18 Szekalska M, Sosnowska K, Czajkowska-Kośnik A, Winnicka K. Calcium chloride modified alginate microparticles formulated by the spray drying process: a strategy to prolong the release of freely soluble drugs. Materials (Basel) 2018;11(09):1522
19 Velings NM, Mestdagh MM. Physico-chemical properties of alginate gel beads. Polym Gels Netw 1995;3(03):311–330
20 Ouwerx C, Velings N, Mestdagh M, Axelos MA. Physico-chemical properties and rheology of alginate gel beads formed with various divalent cations. Polym Gels Netw 1998;6(05):393–408
21 Quong D, Neufeld RJ, Skjåk-Braek G, Poncelet D. External versus internal source of calcium during the gelation of alginate beads for DNA encapsulation. Biotechnol Bioeng 1998;57(04):438–446
22 Puguan JMC, Yu X, Kim H. Characterization of structure, physicochemical properties and diffusion behavior of Ca-alginate gel beads prepared by different gelation methods. J Colloid Interface Sci 2014;432:109–116
23 Swioklo S, Ding P, Pacek AW, Connon CJ. Process parameters for the high-scale production of alginate-encapsulated stem cells for storage and distribution throughout the cell therapy supply chain. Process Biochem 2017;59:289–296
24 Russo R, Malinconico M, Santagata G. Effect of cross-linking with calcium ions on the physical properties of alginate films. Biomacromolecules 2007;8(10):3193–3197
25 Wong TW. Alginate graft copolymers and alginate-co-excipient physical mixture in oral drug delivery. J Pharm Pharmacol 2011; 63(12):1497–1512
26 Loo YY, Rukayadi Y, Nor-Khaizura M-A-R, et al. In vitro antimicrobial activity of green synthesized silver nanoparticles against selected gram-negative foodborne pathogens. Front Microbiol 2018;9:1555
27 Rai M, Yadav A, Gade A. Silver nanoparticles as a new generation of antimicrobials. Biotechnol Adv 2009;27(01):76–83
28 Carlson C, Hussain SM, Schrand AMK, et al. Unique cellular interaction of silver nanoparticles: size-dependent generation of reactive oxygen species. J Phys Chem B 2008;112(43): 13608–13619
29 Schacht VJ, Neumann LV, Sandhi SK, et al. Effects of silver nanoparticles on microbial growth dynamics. J Appl Microbiol 2013; 114(01):25–35

